The behaviour of trough stiffener to crossbeam connections in orthotropic steel bridge decks

J.S. Leendertz
Engineering Division, Ministry of Transport, Public Works and Watermanagement, Zoetermeer,
The Netherlands

M.H. Kolstein
Delft University of Technology, Faculty of Civil Engineering, Delft, The Netherlands

This article describes the behaviour and stress analysis of the crossbeams in orthotropic steel decks
with continuous trapezoidal closed stiffeners. The trough stiffener to crossbeam connections, with or
without cope holes, influence the behaviour of the crossbeam. The effects can be transferred to effec-
tive properties of a beam without cut outs.
The deformations of the crossbeam and the stiffeners cause secondary stresses in the stiffeners and the
web of the crossbeam. The sensitivity of these stresses with respect to various web depths and shapes
of cut out is also investigated.
The objective of this study is to improve the knowledge of the fatigue design of these structures.

Keywords: orthotropic steel bridge deck, trapezoidal closed stiffener, trough stiffener, crossbeam,
stress analysis, fatigue, effective bending stiffness, effective shear stiffness.

1   Introduction

Orthotropic decks are often used in steel bridges. In this type of structure the load carrying functions
of the deckplate, the longitudinal stiffener, the crossbeam and the main girder are integrated.

In the earlier orthotropic steel decks the deckplate was stiffened by angles, bulb stiffeners or strips.
Due to the relative low bending and torsional stiffness of these elements, the spacing between the
crossbeams was usually limited to approx. 2.0 m.
In the past the span of the stiffeners could be increased when closed stiffeners were introduced.
Their bending and torsional stiffness allowed for an increase of the span of the stiffeners up to
approximately 4.0 m. Usually they are made of plate material in thicknesses varying from 6–10 mm
which is rolled or pressed. Fig. 1 shows a perspective view of the underside of an orthotropic deck
and Fig. 2 shows some types of stiffeners.
Inspections nowadays show many small cracks in the details and particularly in the stiffener
connections – crossbeam connections, as shown in Fig. 3. They are supposed to have fatigue as its

main origin. Though many of these cracks as such are not immediately threatening the structural integrity of the bridge as a whole, if propagating, they may develop in such a way or to such locations that in the end they endanger the structural integrity.
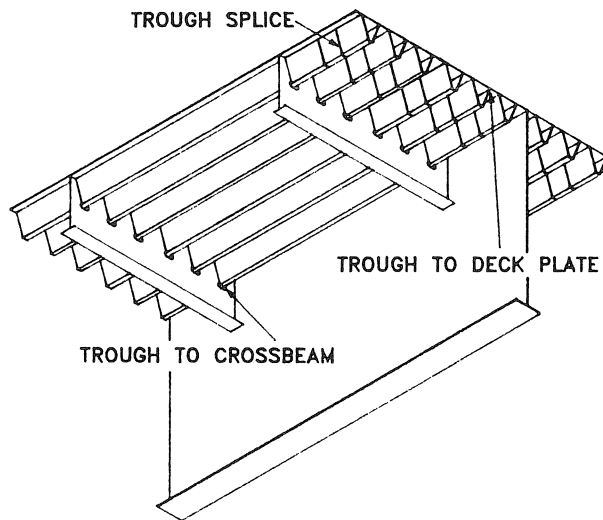

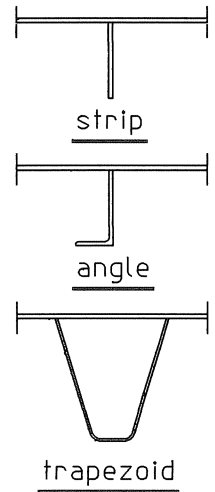Fig. 1. Typical orthotropic steel deck structure.
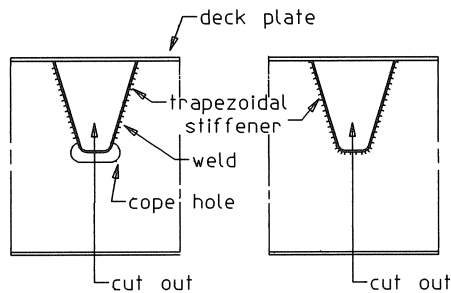

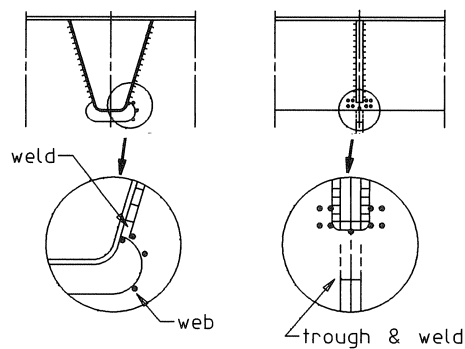Fig. 2. Stiffeners.

Fig. 3. Closed stiffened connections.

Fig. 4. Cracked locations in connections.

In practice this causes frequent repair works to be carried out. In most cases the underside of the steel decks is not easy accessable which makes the repairs expensive. In motorway bridges in the Netherlands the connection between trough and crossbeam web has shown to be the most sensitive location with respect to cracks. This phenomenon forces the attention to the behaviour of the connection. The locations of interest are shown in Fig. 4.

A better knowledge of the behaviour of these details can support the development of adequate repairs and repair techniques. It also can act as a guide for development of better details for future structures.

The behaviour of the connection between stiffeners and crossbeam shows complicated stress distributions, both for open stiffeners and closed stiffeners. Until now the studies concentrated merely on the static behaviour Pelikan, Esslinger [6]; AISC Design Manual for Orthotropic Steel Plate Deck Bridges [9] and on the fatigue behaviour of the free edges of the web.
The behaviour of the crossbeams has previously been analysed by a "Vierendeel" schematisation, a "Multi Column System" and FE-analyses which have been presented by Falke [1] and Mang [8]. The approximate computations show reliable stress results in the narrowest section of the tooth if appropriate stress concentration factors are applied.
However the approximate computations used so far do not give much information about the displacements and the stresses at lower points of the connection between the trough and the crossbeam web as shown in Fig. 4.

The studies on the stress distributions and the fatigue behaviour of these details [1], [3], [4], [8], [10] contribute to understanding the stress distributions at various loadings and to a more integral approach of the fatigue problems in orthotropic decks. This has led to the search for approaches that both describe the behaviour of the crossbeam as a whole with practical equivalent statical values and give the possibility to define the local behaviour of the locations of interest.
In addition they can be a part of a simple approach of the analysis of the deck as a whole.

The knowledge of the sensitivity for various geometrical properties in relation to the mechanical behaviour may indicate the most favourable solutions for the connections in future.

This article deals with the mechanical behaviour of the connections between the continuous trapezoidal closed stiffener (trough) and the crossbeams, in which the closed stiffeners pass through the crossbeam. A distinction can be made between connections with or without a cope hole, see Fig. 3.
In this article effective properties for the crossbeam bending and shear are derived, which enable a simple description for the crossbeam in the structures as a whole. Further it will be shown how secondary in plane effects cause concentrated forces in the connections and how the flexure of the stiffeners by means of rotations causes locally concentrated forces in the connections between crossbeams and stiffeners.

One specific type of crossbeam is analysed for various depths of the web and different widths of the cutout, in order to find the influence of various geometrical aspects of these connections. In addition the span lengths have been varied in accordance with the in plane bending moment capacity.

By means of an analytical frame model the section forces are derived. Based on the section forces, in several locations of interest the displacements and stresses are investigated. In further studies the results from these investigations will be integrated in a more general approach.

In order to verify the validity of the approximate models that were used to carry out hand computations, numerical analyses have been carried out with FE-models. From these models the section forces and moments were determined as well and compared to the results from the hand computations. The used programme was DIANA developed by TNO Building and Construction Research Institute in the Netherlands. The pre- and post processing has been carried out with FEMGEN/FEM-VIEW.

Based on the analyses as presented here which are laid down in a Stevin Report of Delft University of Technology [10], it is envisaged to develop later easy methods for the fatigue design of these details.

If not stated explicitly, all dimensions are in millimeters (mm), forces in Newton (N), stresses in N/mm2 (MPa). This applies to every analysis in this article. The list of symbols is given in Chapter 11. All results discussed are presented in the Annex Tables A1–A26.

2 Behaviour and dimensions of the crossbeam

The behaviour of the crossbeam is analysed, distinguishing between the "in plane" and the "out of plane" effects in the web of the crossbeam, which are separately treated in this article but need to be combined in the analyses of real structures.

2.1 In plane behaviour

The "in plane behaviour" of the crossbeam is strongly affected by the cut outs, which cause the beam to act like a "Vierendeel Girder" as shown in Fig. 5. This schematization applies in particular to the transmission of shear forces.

Compared to trusses the general shear forces are taken by secondary bending and shear in the remaining vertical and horizontal elements.

This already has been stated by many others and is not new as such. However in this study the behaviour of this system is transferred into a global behaviour. Further local relative displacements are derived in order to find the imposed deformations which are relevant for the locations that are sensitive for fatigue. The in plane behaviour is discussed in Chapters 3 to 7.
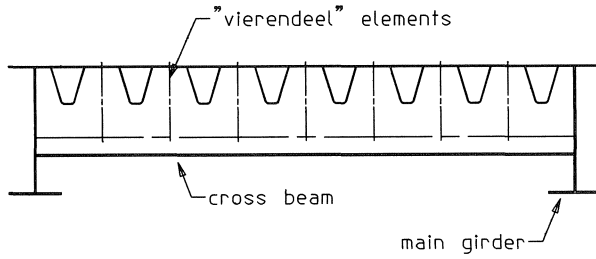
Fig. 5. *"Vierendeel-system" in crossbeam of orthotropic steel deck.*

2.2 *Out of plane behaviour*

Rotations of the deck about the longitudinal axis of the crossbeam generate out of plane bending effects in the web of the crossbeam. Through a schematization with beams (B1, B2, B3) as shown in Fig. 6 the section forces and stresses in relevant locations are computed. Until now this has not yet been included in reported investigations. In Chapter 8 the analysis is further discussed.
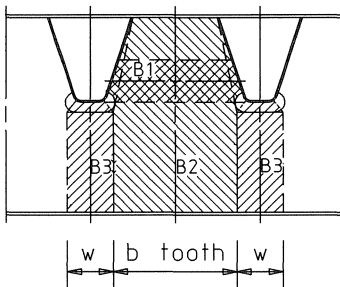

Fig. 6. *Out of plane behaviour.*

2.3 *Investigated dimensions*

In order to investigate the influence of different dimensions, computations have been carried out on 5 beam sections with common dimensions for this type of structures. In these 5 beam types the influence of 5 cut-outs, only varying in width is investigated.

Table 1. Structural dimensions of investigated beams.

Beams

Beam type nr.	Upper flange	Web	Bottom flange	Span standard	Span full bending capacity
1	1400×12	600×10	200×16	7200	7200
2	1400×12	800×10	200×16	7200	8750
3	1400×12	1000×10	200×16	7200	10215
4	1400×12	1200×10	200×16	7200	11635
5	1400×12	1400×10	200×16	7200	13030

As is shown in Table 1 beam type nrs. 2–5 have been considered for two spans, the *Span standard* and the *Span full bending capacity*. The reason for this is the following: In practice designers will use deeper beams for longer spans, because of the increased bending moment capacity. Generally spoken the bending capacity of the beam increases linearly with the quotient of the resistance moments W_n/W_1 if the bending stress in the bottom flange for the full web crossbeams is taken as a reference. The computations have been carried out for simple spans, so the bending moment in type "n" is:

$$M = \tfrac{1}{8} \cdot q \cdot l_n^2 \tag{1}$$

Then the bending stress in the bottom flange is:

$$\sigma_b = \frac{q \cdot l_n^2}{8 \cdot W_n} \tag{2}$$

Taking the beam with a span of 7200 mm with W_1 as a reference, than the span with respect to the full bending capacity for beam type "n" can be found by:

$$l_n = l_1 \cdot \sqrt{\frac{W_n}{W_1}} \tag{3}$$

which means that in beam type "n" the bending moment M_n will be:

$$M_n = M_1 \cdot \frac{W_n}{W_1} \tag{4}$$

and the shear force S_n will be:

$$S_{vn} = S_{v1} \cdot \sqrt{\frac{W_n}{W_1}} \tag{5}$$

Table 2. Dimensions of cut outs with cope holes.

Depth			Width		
350	$w = 75$	$w = 125$	$w = 175$	$w = 225$	$w = 275$

Table 2 shows the different cut outs that are investigated. The former FKH profile 2/325/6 which is used with a cope hole width of 175 mm is taken as a basis for the investigations, varying the with of the cope hole. For the analytical model straight edges have been assumed using the outer boundaries of the cope hole as a guide (w). Fig. 8 shows the idealization.
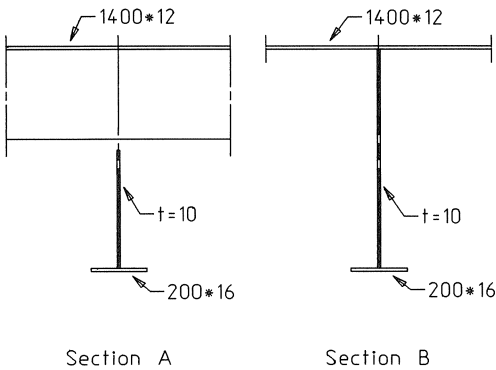

Section A   Section B

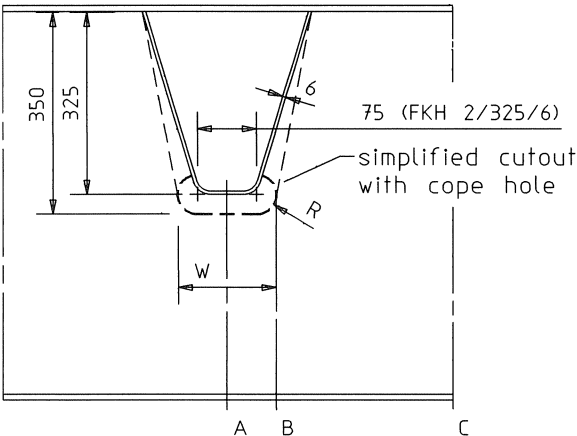Fig. 7. Dimensions of beam sections.

Fig. 8. Simplified cut out.

3   Crossbeam in plane bending mechanism

3.1   Analytical model in plane bending

Fig. 9 shows the side view of a relevant part of the structure. Due to the absence of material at the cut outs the crossbeam consists of sections where upper flange, web and lower flange are present and act like an I-beam (Part II, between Sections B and C) and sections where only a flange and a T-beam are present, but not connected (Part I, between Sections A and B).
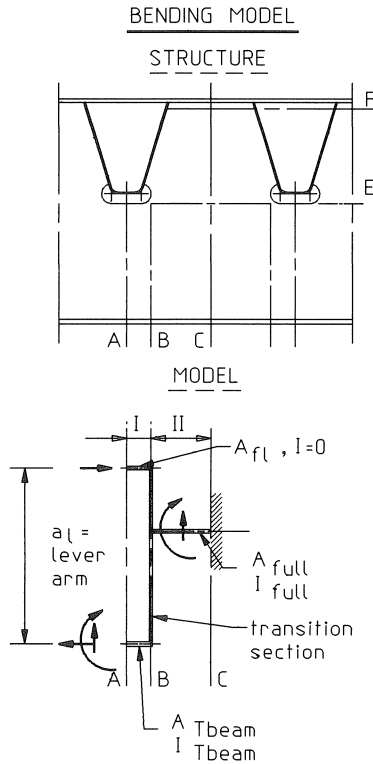
Fig. 9.   Analytical model in plane bending.

The shear forces in Part I are taken by the T-beam and the bending moment is taken by a lever system and a secondary bending moment. The bending stiffness of the deck is negligible. In Part II the beam acts as an I-beam.
In the idealization a transition section (Section B) is assumed connecting Part I and II.
With this schematization the influence of the cut outs on the overall bending stiffness of the cross-beam will be derived. The stiffness ratio between the beam with cut outs and without cut outs is called: equivalent bending stiffness ratio (c_b).

If a unit moment is applied in Section A on the lever system, the rotation angle (ϕ_1) with respect to Section B can be computed. The T-beam is forced to have the same rotation angle. This causes a secondary bending moment in the T-beam. The unit moment with the added secondary bending moment can be applied on Part II, thus causing a rotation (ϕ_2) of Section B with respect to Section C and giving an additional rotation to Section A.

The rotation of Section A (ϕ_A) can also be computed for the case that both Part I and Part II possess the full I-section.

Based on the comparison of these results for Section A, the effect of the cut out with cope hole can be computed.

The stiffness of the beam with cut outs can be related to the stiffness of the beam without cut outs by means of the effective bending ratio ($c_b = \phi_A$ – without cut outs – / ϕ_A - with cut outs –).

The procedure of computations as described above is as follows:

1. Applying the unity moment on Part I with length l_I gives:

$$\phi_1 = \frac{1}{a_I}\left[\frac{M_{\text{unity}} \cdot l_I}{a_I \cdot E} \cdot \left(\frac{1}{A_{fl}} + \frac{1}{A_{\text{T-beam}}}\right)\right] \tag{6}$$

2. The secondary moment in the T-beam can be determined, based on the same rotation:

$$M_{\text{T}-beam} = \frac{E \cdot I_{\text{T-beam}} \cdot \phi_1}{l_I} \tag{7}$$

3. The rotation over Part II with length l_{II} is determined by:

$$\phi_2 = \frac{(M_{\text{unity}} + M_{\text{T-beam}}) \cdot l_{II}}{E \cdot I_{\text{full}}} \tag{8}$$

This means that the rotation in Section A with respect to Section C is:

$$\phi_A = \phi_1 + \phi_2 \tag{9}$$

4. The rotation in Section A in case a full web is present, is computed by:

$$\phi_A = \frac{(M_{\text{unity}} + M_{\text{T-beam}}) \cdot (l_I + l_{II})}{E \cdot I_{\text{full}}} \tag{10}$$

The rotations in Section A for a crossbeam with a full web and a crossbeam with cut outs can be related by the equivalent bending stiffness ratio c_b in the following way:

$$c_b = \frac{\phi_{\text{A-full}}}{\phi_{\text{A-cutout}}} \tag{11}$$

The equivalent bending stiffness ratio shows the sensitivity of the general bending stiffness of the crossbeam for cut outs. It gives no information on the stresses in the various sections.

As an intermediate result after computations 1 and 2 the lever system ratio R_l is found:

$$R_l = \frac{M_{\text{unity}}}{M_{\text{unity}} + M_{\text{T-beam}}} \tag{12}$$

Further the T-beam ratio, R_T can be derived by:

$$R_T = \frac{M_{\text{T-beam}}}{M_{\text{unity}} + M_{\text{T-beam}}} \tag{13}$$

For a known bending moment in Section "A", the distribution to the lever system and the secondary bending in the T-beam can be computed through the lever system ratio (R_l) [12] and the T-beam ratio (R_T) [13].

3.2 *Numerical bending verification model*

Fig. 10 shows the numerical bending verification model. The web of the structure is modelled with shell elements. Two versions have been modelled: one with a full web and one with a cut out.

The deckplate and the bottom flange are modelled with line elements. The mid section of the trough (Section A) is clamped and the centreline of the tooth (Section C) is given a unit rotation. Acting so, the reactions in relation to the rotation of Section A can be related to the results obtained by the analytical model. The results in Section A allow to find the contributions of the lever system and the secondary bending as well.
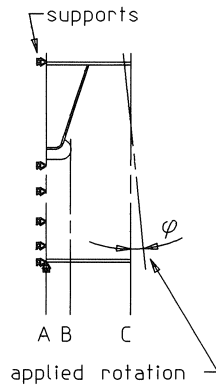

Fig. 10. *Numerical model in plane bending.*

When the results were interpreted the contraction effect showed to play an important role in the higher crossbeams. It causes additional vertical displacements in a section which are not envisaged in a 2-D Bar schematization. Moreover the transition section plays a role. It will not remain perfectly

226

straight as considered in the analytical model. The T-beam can not be regarded as being fully clamped in the transition section. These effects may not be neglected as such, but can not easily be integrated in the analytical model which is based on a line element schematization.

3.3 Results

The numerical models show a sensitivity for the width of the cut out, which is not found in the analytical models. The reason for this can be found in the different capabilities of the models. The T-beam in the numerical model is not fully clamped in Section B and in analyses proved to be sensitive to the contraction effect. The analytical model is in fact only based on statical values of the sections.

In the analytical models every beam type shows the same value for the T-beam ratio R_T, varying from 0.019 to 0.179 for $H = 600$ and $H = 1400$ respectively. The results from the FE-analyses vary from 0.014 to 0.180. The scatter becomes smaller for higher beams.

The equivalent bending stiffness ratios for c_b the analytical models are varying from 0.98–1.00. The results of the FE-analyses vary from 0.99 to 0.93. It is clear that the line element approach in the analytical models is less accurate for higher T-beams.

Based on the results in the tables the following conclusions can be drawn:

1. The FE-models react weaker than the hand calculations, which effect is found more strongly in the higher crossbeams.

2. The deviation between results for c_b in FE-models and "hand" calculations is larger in higher webs. This can be explained by the fact that the line element description does not apply to higher T-beams.

3. In general the cut out does not very strongly affect the overall bending stiffness.

4 Crossbeam in plane shear mechanism

4.1 Analytical model in plane shear

Very often the cutouts in crossbeams are of substantial dimensions in comparison to the beam as a whole. This affects the shear force system of the crossbeam considerably. The effects of the cut outs with respect to shear have been investigated by Falke [1] and Haibach [7] using a "Vierendeel Schematization" as a basis.

With a "Vierendeel Schematization" as a starting point and deriving the deformations of the part between centre lines of two troughs, an "Equivalent Web Thickness Ratio" (c_s) can be derived. This can be used for the determination of the global shear stiffness and deflections of the crossbeam.

Fig. 11 shows the part of the crossbeam and the schematization. Like in Chapter 3, the structure is divided into rigid parts and deforming parts. The middle part (Part II, l_{II}) is assumed to be rigid, the reason for this is explained below. The parts below the cut outs are assumed to deform in a vertical direction (Part I, l_I) between Section A and B and (Part III, l_{III}) between Section B and C. The tooth (Part IV, l_{IV}) between Section E and F is assumed to deform in a horizontal direction.

SHEAR MODEL
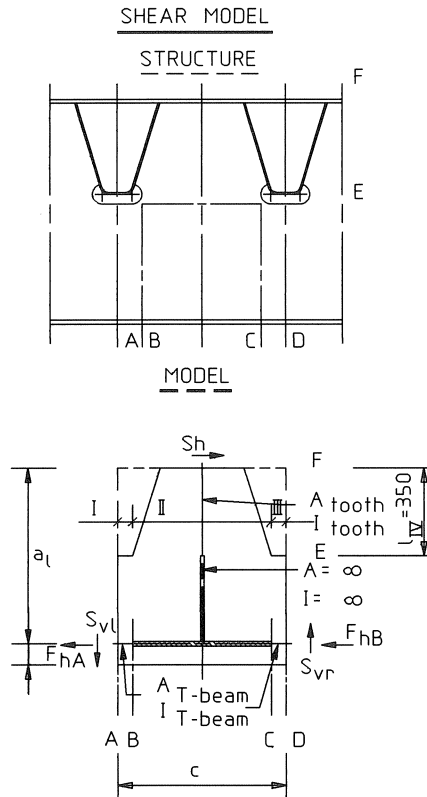
STRUCTURE

MODEL

Fig. 11. Analytical model in plane.

This (upside down) T-frame structure of bars is loaded along the left side by a vertical unit shear force (S_{vl}) and along the right side by the same unit shear force of opposite sign (S_{vr}). In order to ensure the equilibrium of moments, a related horizontal force must be applied in Section F (S_h). The vertical equilibrium is fulfilled by the chosen forces, the horizontal equilibrium is fulfilled by the difference of horizontal forces in Section A and D, F_{hA} and F_{hB} respectively.

The stresses caused by S_{vl} and S_{vr} (see Fig. 11) are such, that at the locations where they interact with the stresses from S_h the signs of perpendicular stresses are the same, which effect restrains the deformations and causes a more rigid behaviour due to the contraction effect (Poisson's ratio). Part IV can not be regarded as an I-beam with the trough web acting as a flange with an effective web thickness for the tooth. In Section E where the highest bending effect occurs, a cope hole causes the absence of a connection and in case of a fully welded around connection, the effective width is reduced to almost "0" by the curvature in the bottom of the trough.

The determination of the effective web thickness ratio is carried out, according the following steps:

a. Determination of S_h

The equilibrium of moments of the vertical shear forces leads to:

$$S_h = \frac{S_{vl} \cdot 0.5c + S_{vr} \cdot 0.5c}{a_1} \tag{14}$$

b. Determination of the deformations in the tooth

$$\delta_h = \frac{S_h \cdot l_{IV}^3}{3 \cdot E \cdot I_{tooth}} + \frac{S_h \cdot l_{IV}}{G \cdot A_{tooth}} \tag{15}$$

c. Determination of the deformations in the T-beam, Part I:

$$\delta_{vl} = \frac{S_{vl} \cdot l_I^3}{3 \cdot E \cdot I_{T\text{-beam}}} + \frac{S_{vl} \cdot l_I}{G \cdot A_{T\text{-beam}}} \tag{16}$$

$$\delta_{vr} = \frac{S_{vr} \cdot l_{III}^3}{3 \cdot E \cdot I_{T\text{-beam}}} + \frac{S_{vr} \cdot l_{III}}{G \cdot A_{T\text{-beam}}} \tag{17}$$

In Fig. 12 the local deformations of the parts I, III and IV due to the relevant external forces are shown. The contributions from bending and shear in the tooth according to step "b" vary from 0.41/0.59 (bending/shear) to 0.64/0.36.

In step "c" the same analyses have been carried out for the T-beams. The contributions from bending and shear vary from 0.14/0.86 (bending/shear) to 0.00/1.00. The highest contribution from bending is found in the beams with the widest cut outs. The shear deformation shows to be the most important contribution in most of the investigated beams. The effect of neglecting the bending component in the determination of the relative vertical displacements of the lower ends of the trough to web connection will be investigated later.

d. Transfer of horizontal tooth deformations into vertical deformations

The vertical shear deformations in beams are determined using the shear force, the web area, the length and the shear modulus (G). Working towards equivalent descriptions, the tooth deformations have to be transformed into vertical deformations of the T-frame between Section A and Section D.
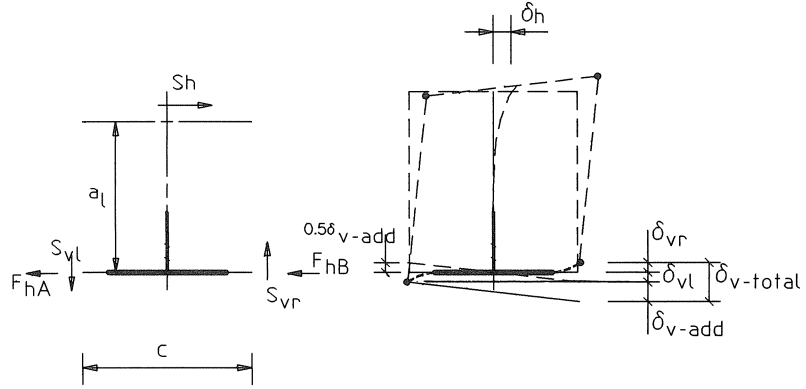
Fig. 12. Forces and displacements due to shear.

Contribution $\delta_{\text{v-add}}$ due to horizontal deformations of tooth:

$$\delta_{\text{v-add}} = \frac{\delta_{\text{h}} \cdot c}{a_1} \qquad (18)$$

$$\delta_{\text{v-total}} = \delta_{\text{vl}} + \delta_{\text{vr}} + \delta_{\text{v-add}} \qquad (19)$$

The contributions from the T-beams (V) and the tooth (H) to the total vertical deformation are varying from 0.15/0.85 (V/H) to 0.28/0.72. for $H = 1400$ to $H = 600$ respectively. The contributions from the T-beams (V) and the tooth (H) show a relative sensitivity for the width of the cut out. The web depth of the beam shows a smaller influence. Anyhow it is not possible to neglect one of the contributions from the T-beam and or the tooth.

As shown above, in most cases the largest contribution in the deformation $\delta_{\text{v-total}}$ is generated by the horizontal deflections of the tooth. With respect to δ_{h} of the tooth, both contributions from bending and from shear are relevant. In the T-beam the bending deformations play a minor role.
The contribution from the bending in the T-beam (B), the contribution of the T-beam (V) results in the combined effect in the assembly ($B \cdot V$), the T-beam bending contribution is shown to vary from 2.8%–4.4% in the investigated beams. The average value is 3.7% of the whole vertical deformation, which may be considered to be neglected.

230

w	$H = 1400$	$H = 1200$	$H = 1000$	$H = 800$	$H = 600$
75	0.91	0.84	0.78	0.71	0.61
125	0.71	0.67	0.61	0.55	0.47
175	0.55	0.52	0.47	0.43	0.36
225	0.43	0.4	0.37	0.33	0.28
275	0.3	0.3	0.27	0.25	0.21
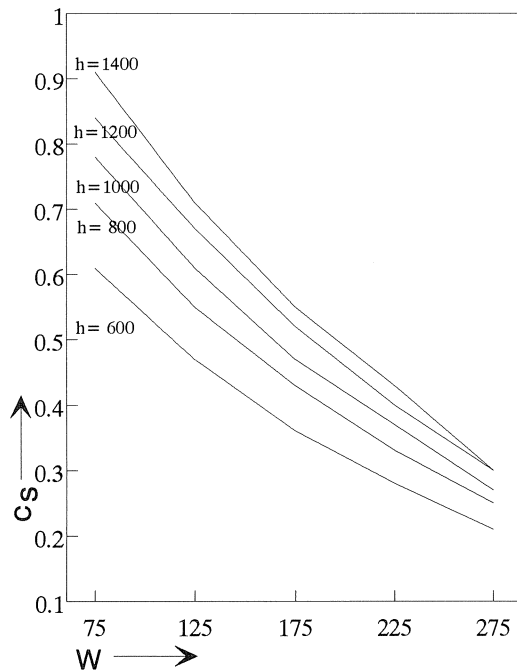
Fig. 13. Equivalent shear stiffness ratio.

e.   Equivalent Shear Stiffness Ratio

The equivalent shear stiffness ratio (c_s) can be derived from the vertical deformations in a structure with cut outs, in relation to a structure with a full web. It is determined as follows:

Let be $S_v = S_{vl} = -S_{vr}$, then the vertical displacement between Section A and D for a beam with a web without cut outs is:

$$\delta_{v\text{-full}} = \frac{S_v \cdot c}{G \cdot A_{web}} \qquad (20)$$

231

The equivalent shear stiffness ratio (c_s) can be found by:

$$c_s = \frac{\delta_{v\text{-full}}}{\delta_{v\text{-total}}}$$

(21)

4.2 Results

The results determined according to the procedure as mentioned above vary from 0.91 to 0.21 for Beams $H = 1400\ w = 75$ to $H = 600\ w = 275$ respectively. The width of the cut out has a stronger effect than the beam depth, but in all cases the effect plays an important role.(c_s for $w = 275$/ c_s for $w = 75$ is approx. 0.33) and (c_s for $H = 600$/c_s for $H = 1400$ is approx. 0.70)

4.3 Numerical shear verification model

Fig. 14 shows the FE-model used for verification. The web is modelled with shell elements, the bottom flange is modelled with line elements. The model is supported horizontally and vertically, at the top and bottom of the centre line of the tooth. The end sections of the web left (A) and right (D) are forced to remain straight under loading, but are free to deflect and rotate.
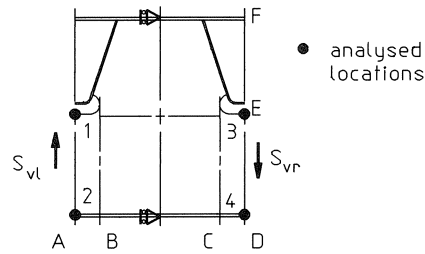

Fig. 14.   Numerical model in plane shear.

The sections in the centre lines of the troughs are loaded. This means that the deflections immediately give information about the shear stiffness of the whole section as the bending and shear of the tooth is automatically included. Special attention has been paid to the contraction effect, which causes different vertical displacements at the top and bottom of the T-beams and different horizontal displacements in Sections A and D. In real structures the contraction effect in these sections is restrained by material at the other side. For the interpretation the average values of the displacements at the top and the bottom have been considered.

4.4 Results of numerical model

The results from the FE-analyses vary from 0.62 to 0.18 for beam $H = 1400\ w = 75$ and beam $H = 600$ $w = 275$ respectively. The average value due to the sensitivity for the cut outs: c_s for $w = 275$ divided by c_s for $w = 75$ is approx. 0.38, the sensitivity for the beam depth is: c_s for $H = 600$/ c_s for $H = 1400$, approximately 0.63.

4.5   Comparison analytical model and FE-analyses.

The wider the cut outs and the deeper the beams, the better the values do coincide. The effect of widening the cut out and enlarging the web depth shows approximately the same relationship for both analyses. A deeper investigation showed that the contraction effect leads to disturbing effects on the results. The introduction of the bending in the T-beam in the crossbeams with smaller cut outs is in reality more restrained than could be simulated in the FE-models. It can be explained as follows: The section below the trough will not show an elongation or compression as observed in these FE-models due to the fact that the compression of one side is restrained by the elongation of the other side to which it is connected. (Antimetric Structural Behaviour) These effects play a larger role in beams with small cut outs.

The following conclusion can be drawn:
–   The mechanism acts as supposed, but the FE models act somewhat weaker.

5   External loads

Accumulated horizontal shear forces establish the bending moments in the beam.

Due to the behaviour of the structure it is necessary to distinguish between: a.) Centric loading on the tooth, which occurs in road traffic bridges by equally distributed loads and wheel loads on the deck between the troughs. b.) Eccentric loading on the tooth which is caused by centric loading of a trough. c) Combinations of a. and b.
The transfer of the external loads causes additional stresses in Section E, which may not be neglected. In real structures the loading pattern will be a mixture of these loadings.

Fig. 15.   External loads on the shear model.

The behaviour will be analysed with a schematization which is similar to Chapter 4.
The shear forces, as displayed in Fig. 15 are the result of external loads on the crossbeam. In the case of equally distributed loads every tooth contributes with the same magnitude.

233

These loads can be considered acting centric on a tooth ($e = 0$). Then the equilibrium of the vertical shear forces becomes:

$$S_{vl} = S_{vr} + P_v \tag{22}$$

And S_h results from:

$$S_h = 2 \cdot \frac{S_{vr} \cdot 0.5c}{a_l} + \frac{P_v \cdot 0.5 \cdot c}{A_l} \tag{23}$$

In Section E this leads to a normal force N:

$$N = P_v \tag{24}$$

and a bending moment M:

$$M = S_h \cdot l_{IV} \tag{25}$$

The stresses in Section E, as shown in Fig. 15 can be derived from expressions [24] and [25] using the appropriate stress concentration factor.
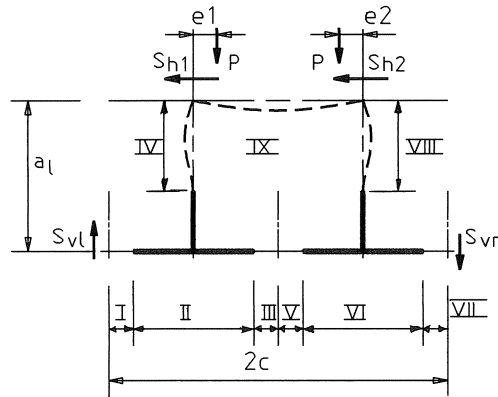
Fig. 16.   Arrangement of stiffnesses and local forces.

If external loads are applied which act eccentrically ($e = \neq$) the antimetric behaviour of the system tooth with T-beam is affected in such a way that a local framework as shown in Fig. 16 becomes active. Again the schematization is an extension of the shear model as used in Chapter 4. The two adjacent teeth (IV, VIII) establish together with the deckplate (IX), the rigid parts (II, VI) and the T-beams (I, III, V, VII) a frame. This frame as a whole introduces S_h:

$$S_h = S_{h1} + S_{h2} \tag{26}$$

234

The contributions S_{h1} and S_{h2} depend on the respective stiffnesses of the elements of the frame. Theoretically a complete different behaviour is expected, but the FE analyses of a complete cross-beam with large external loads [ref. 4], which are not further discussed here, show that the stress pattern in case a trough was loaded centrically, did not not differ very much from a trough loaded eccentrically. Further investigations are required for the development of a simple schematization.

6   Imposed deformations by in plane crossbeam bending and shear

In most structures the load carrying parts do influence other parts by imposed deformations. They cause normal forces, bending moments and shear forces, for which they originally have not been designed.
Fig. 17 shows the crossbeam-closed stiffener connection with a cope hole under imposed deformations, which effect is most obvious at the two lower ends of the connections with the same trough.

DEFORMATIONS OF COPE HOLE
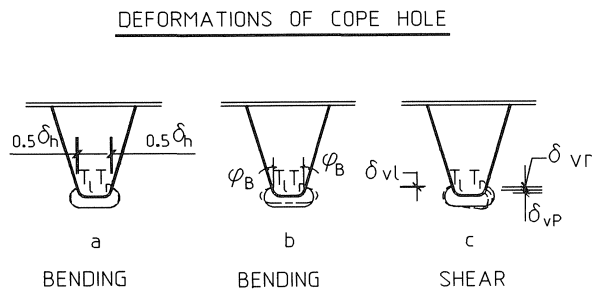
Fig. 17.   Deformations of cope hole.

6.1   Mechanisms and schematizations

Bending in the crossbeam causes a relative horizontal displacement (see Fig. 17a) and symmetrical rotations (see Fig. 17b) in these locations and shear causes a relative vertical displacement (see Fig. 17c) in these locations.

In Fig. 18 is shown how these displacements force the bottom part of the trough to behave like a small frame structure under various imposed displacements and rotations.
The horizontal displacements and rotations due to bending cause symmetrical bending in the frame and the vertical displacements due to shear cause antimetrical bending. Fig. 19 shows the schematization. Because of the displacements imposed, it is possible to simulate the symmetrical and antimetrical imposed displacements with loadings on cantilever systems, clamped in the cross-beam web at locations T_l and T_r.
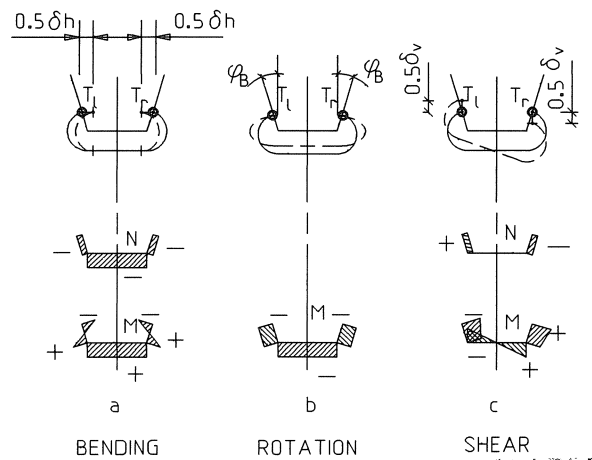
235

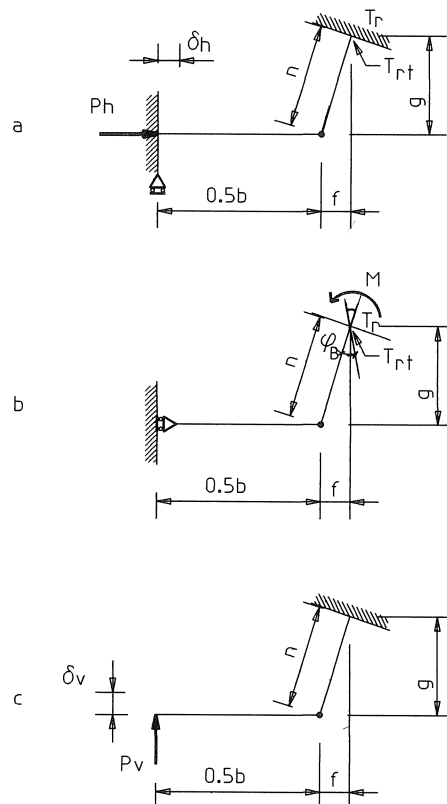Fig. 18. Simple frame loadings and deformations.

Fig. 19. Simplified loads on partial frames.

236

The simplifications are justified by the following assumptions:

– Difference in rotations in both frame supports due to crossbeam shear is negligible.
– The torsional and distorsional stiffness as well as the bending stiffness carry over effect to other crossbeams are of minor importance.

The latter assumption applies as long as the behaviour of the crossbeam as such is studied. The carry-over effect between adjacent crossbeams with different deflections and rotations is not part of these studies, but can be introduced later.
Further the influence of external loads is mentioned, but not taken into account in these computations.

The magnitudes of the displacements can be derived, using the analytical models from Chapters 3, 4 and 5. In the displacements caused by shear the influence of the local bending deformation of the T-beam is neglected, which will generally cause an underestimation of the displacements of 4% as mentioned in chapter 4.

In real structures the frame has curved corners. The bottom of the trough is schematized as a trapezoidal frame with an estimated effective width. The results will therefore not be exact, but the tendencies in the results can be considered to be reliable.
The following procedure describes how the displacements are computed and from there the section forces and nominal stresses. Later this procedure can be completed by stress concentration factors which then give the hot spot stresses.

6.2   Crossbeam bending

a.   Horizontal displacements caused by crossbeam bending

Fig. 20 shows the part of the structure with the relevant elements and their movements. The T-beam is subjected to bending and the rotation (ϕ_B) in Section B can be computed. The relative displacements of T_l and T_r are found if the distance between these locations and the neutral axis of the T-beam is used ($a_l - l_{IV} + d_c$).
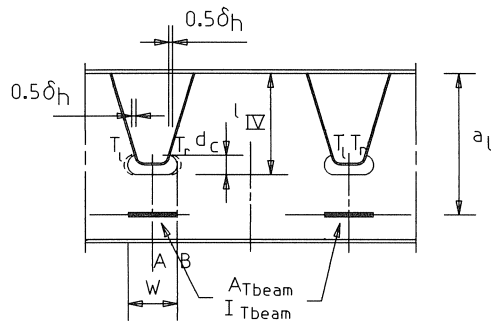

Fig. 20.   Elements for horizontal displacements in relation to crossbeam bending.

$$\delta_{\mathrm{h}} = 2\left(\frac{M_{\mathrm{lever}} \cdot 0.5w}{a_{\mathrm{l}} \cdot E \cdot A_{\mathrm{T\text{-}beam}}} - \frac{M_{\mathrm{T\text{-}beam}} \cdot 0.5 \cdot w \cdot (a_{\mathrm{l}} - l_{\mathrm{IV}} - d_{\mathrm{c}})}{E \cdot I_{\mathrm{T\text{-}beam}}}\right) \tag{27}$$

b. Frame deformations due to a horizontally applied unit force

Fig. 19a shows the horizontal deformations (δ_{h}) of the frame by a horizontal force (P_{h}). Once P_{h} is known, the axial support reaction (P) and the bending moment (M) at the support T_{r} can be computed.

$$\delta_{\mathrm{h}} = 2P_{\mathrm{h}}\left(\frac{n \cdot g^2}{3 \cdot E \cdot I_{\mathrm{frame}}} - \frac{n^2 \cdot g^2}{(0.5b + n) \cdot 4 \cdot E \cdot I_{\mathrm{frame}}}\right) \tag{28}$$

At support T_{r}:

$$P = \frac{f}{n} \cdot P_{\mathrm{h}} \tag{29}$$

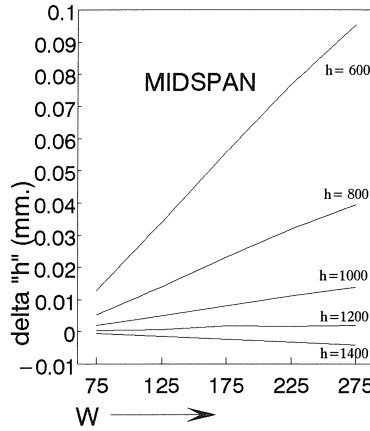$$M = P_{\mathrm{h}} \cdot g - \frac{P_{\mathrm{h}} \cdot g \cdot n}{2\,(0.5b + n)} \tag{30}$$

Fig. 21. Relative horizontal displacement of lower ends of the connection.

Fig. 21 shows the relative horizontal displacements δ_{h} between T_{l} and T_{r}. The computations have been carried out for a midspan bending moment on the crossbeam with $H = 600$ with a magnitude of 7.00E8 Nmm as mentioned in chapter 2. This will generate a working stress in the bottom flange of 240 N/mm^2. In relation to this moment it is possible to derive the maximum bending moments for the other beams types and the shear forces accordingly, under the assumption of equally distributed loads and the spans being simply supported.
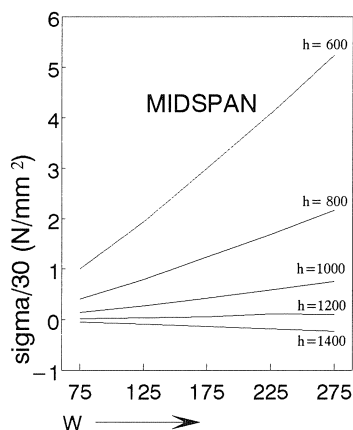
238

Fig. 22. Relative nominal stresses in through wall due to displacements by crossbeam bending.

According to the method as described before, the bending moments and normal forces at the support of the leg of the frames have been computed. Where the locations T_1 and T_r are situated above the neutral axis, compression of the frame is involved and a compression force will occur. The stresses at the outside of the trough wall at the support T_{lt} and T_{rt} will both be compression. In the beam type 1, with $H = 600$ $w = 75$ the locations T_1 and T_r are below the neutral axis so the stresses at the outer fibre of T_{lt} and T_{rt} will be in tension with a magnitude of 30 N/mm^2.

Fig. 22 shows the nominal stresses in the trough web. The values are divided by 30, thus enabling easy comparison between all beams and details with $H = 600$, $w = 75$ as a reference.
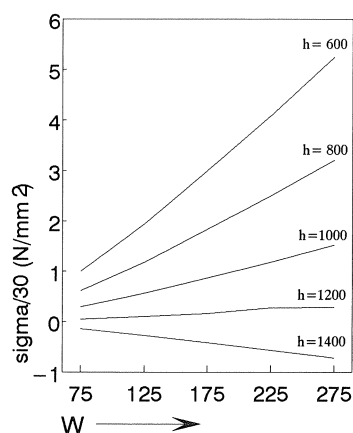

Fig. 23. Relative nominal stresses in beams with fully used bending capacity.

The results in Fig. 22 are based on the assumption that higher beams are used for the same bending moment. In real structures designers will use higher crossbeams for larger spans. In this case the spans can be derived from the resistance moments (W_n/W_1), as described in Chapter 2.

If applied to the values in Fig. 22, the displacements are changed. The stresses are modified accordingly and are shown in Fig. 23.

239

As shown in Fig. 17 in addition to the horizontal displacements the locations T_1 and T_r are rotated as well. The same rotation ϕ_B as used for the determination of the horizontal displacements can be used to derive the additional stresses due to rotation.

Fig. 24 shows the results of the rotations (rad.) which in the beam types investigated vary from 1.309E-5 to 3.302E-4 for $H = 1400$ $w = 75$ to $H = 600$ w=275 respectively. The beam with $H = 1400$ shows a rotation which is 14.5% of the rotation at $H = 600$
If the spans are increased in accordance with the bending moment capacity the results become: 4.290E-5 to 3.302E-4 for $H = 1400$ $w = 75$ to $H = 600$ $w = 275$ respectively. Now the beam with $H = 1400$ shows a rotation which is 47.2% of the rotation at $H = 600$.

The bending moment in the frame at T_{rt} can be computed, based on the imposed rotation:

$$\phi_B = \frac{M}{E \cdot I} \cdot \left[(0.5b + n) - \frac{(b+n)^2}{2 \cdot (b + \frac{2}{3} \cdot n)} \right] \tag{31}$$

Further P_h becomes:

$$P_h = M \cdot \frac{(b+n)}{g \cdot (b + \frac{2}{3}n)} \tag{32}$$

The axial force P in the leg of the frame becomes:
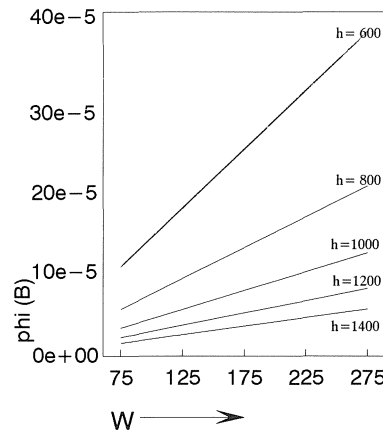
$$P = \frac{f}{n} \cdot P_h \tag{33}$$

Fig. 24. Rotation of Section A with respect to centre of cut out.

Once the section forces are known the stresses can be determined.
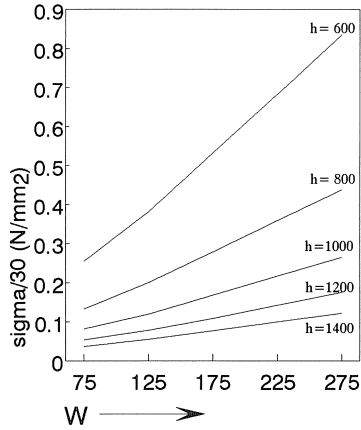
Fig. 25. Relative nominal stresses due to section rotations by crossbeam bending.

In simple span beams the relative horizontal displacement causes an elongation or shortening of the distance between T_{lt} and T_{rt} and leads to tension or compressive stresses in the outer fibre of the trough wall depending from the position in relation to the neutral axis, the rotation always causes a tension stress at the locations T_{lt} and T_{rt}.

The nominal stresses, divided by 30, are shown in Fig. 25. The results for the standard beams vary from 0.037 to 0.837 for $H = 1400$ $w = 75$ to $H = 600$ $w = 275$ respectively.
The results for the beams with varying span lengths, which are not shown in full, vary from 0.123 to 0.837 for $H = 1400$ $w = 75$ to $H = 600$ $w = 275$ respectively.

With respect to the combined stresses in T_{lt} and T_{rt}, the following conclusions can be drawn:
1. A wider cut out leads to higher combined stresses. The diminishing rigidity of the frame is overruled by the increase of the deformations.
2. An increasing depth of the crossbeams reduces the relative displacement of locations T_l and T_r due to the changing position of the neutral axis. This also may cause a change of sign where elongation becomes shortening and has a higher value than the effect of rotation ϕ_B.
3. In addition to the effect under 2. the increase in depth causes a reduction of the elongation/ compression due to the higher stiffness of the beam over the cut outs.
4. The computations for spans in accordance with the bending capacity shows an higher stresses. However the effect of the web depth still governs the results.

The following observation can be made:
In the formula [28] which shows the relationship between δ_h and P_h, the factor $g \cdot n^2$ can be put before the brackets. This means that the leg length n has at least an influence of $g \cdot n^2$ on the stress results. Because of this strong effect, reduction of the stresses mentioned above may be expected if the leg length n is increased.
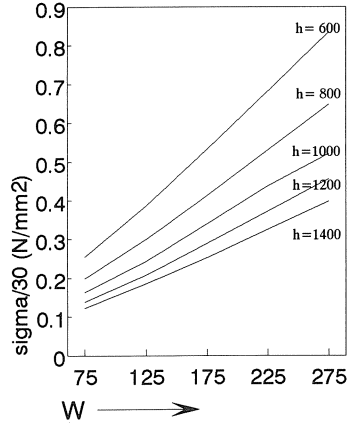
241

Fig. 26. *Relative nominal stresses due to section rotations in spans with fully used bending capacity.*

6.3 Crossbeam shear

Fig. 27 shows the mechanisms for the determination of the relative vertical displacements of locations T_1 and T_r. The shear forces will cause both horizontal and vertical displacements. The relative horizontal displacements depend on the sign of the shear force S_h in each tooth, which will in most cases act in the same direction and be of approximately the same magnitude.
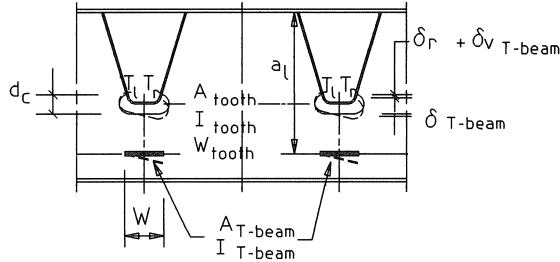

Fig. 27. *Mechanisms for vertical displacements.*

a. Vertical displacements caused by crossbeam shear

The relative vertical displacement in T_1 caused by shear S_v in the T-beam and shear S_h in the tooth can be computed with:

$$\delta_{v1} = \frac{S_v \cdot 0.5 \cdot w}{G \cdot A_{\text{T-beam}}} + \frac{S_h \cdot (l_{\text{IV}} - 0.5 d_c) \cdot d_c}{E \cdot W_{\text{tooth}}} \tag{34}$$

242

The relative vertical displacement in T_r caused by shear S_v in the T-beam and shear S_h in the tooth can be computed with:

$$\delta_{vr} = \frac{S_v \cdot 0.5 \cdot w}{G \cdot A_{\text{T-beam}}} + \frac{S_h \cdot (l_{IV} - 0.5 d_c) \cdot d_c}{E \cdot W_{\text{tooth}}} \tag{35}$$

In presence of an external vertical load P_v which causes in Section E a normal force N and an eccentricity moment M, δ_v is reduced or increased by the following:

$$\delta_{vP} = \frac{N \cdot d_c}{E \cdot A_{\text{tooth}}} + \frac{M \cdot d_c}{E \cdot W_{\text{tooth}}} \tag{36}$$

This effect is not investigated in the computations below.

b.   Frame deformations in relation to crossbeam shear

The vertical displacements in a half frame as shown in Fig. 19c, which through appropriate boundary conditions simulates a complete frame under antimetric vertically imposed displacements can be computed by:

$$\delta_v = \frac{P_v \cdot b^3}{24 \cdot E \cdot I_{\text{frame}}} + \frac{P_v \cdot b \cdot n}{4 \cdot E \cdot I_{\text{frame}}} \cdot \left(\frac{f}{3} + \frac{b}{2}\right) + \frac{P_v \cdot \left(\frac{b}{2} + f\right) \cdot n}{2 \cdot E \cdot I_{\text{frame}}} \cdot \left(\frac{2}{3} \cdot f + \frac{b}{2}\right) \tag{37}$$

This vertical displacement (δ_v) is half of the total relative vertical displacement between T_l and T_r. At support (T_r):

$$P = P_v \cdot \frac{g}{n} \tag{38}$$

$$M = P_v \cdot \left(\frac{b}{2} + f\right) \tag{39}$$

In the computations the beam $H = 600$, $w = 75$ with a span length of 7200 mm. is loaded by a midspan bending moment of 7.00E8 Nmm, which corresponds with a a shear force as a result of equally distributed loads of: $S_v = 3.893e5$ N, as discussed in Chapter 2.

This leads to the relative vertical displacement of T_l with respect to T_r as shown in Fig. 28.

The results show that within the beam types investigated, the effects of larger cut outs are of the same magnitude as smaller web depths.

In the next step the bending moments and the normal forces in the leg of the frame representing the local out of plane behaviour at the locations T_{lt} and T_{rt} of the trough have been computed.

The stresses at the outer side of the trough are tension due to bending and compression due to the normal force on one side and the opposite on the other, in relation to the diagrams of normal forces and bending moments as shown in Fig. 18c.
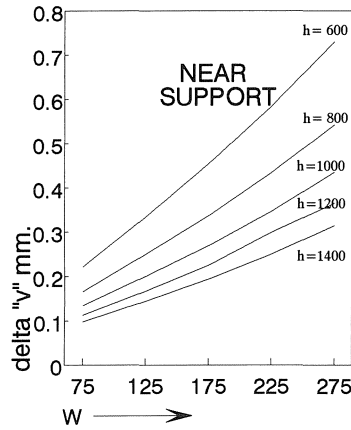
Fig. 28. Relative vertical displacements of T_1 and T_r due to shear.

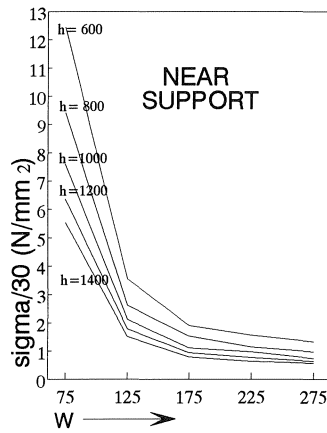| w	$H = 1400$	$H = 1200$	$H = 1000$	$H = 800$	$H = 600$
75	5.53	6.358	7.583	9.404	12.45
125	1.513	1.788	2.119	2.616	3.543
175	0.783	0.947	1.114	1.52	1.897
225	0.642	0.778	0.972	1.146	1.556
275	0.573	0.633	0.745	0.977	1.321

Fig. 29. Relative nominal stresses in T_{lt} and T_{rt}.

Their values are shown in Fig. 29. The stresses are displayed as a factor of 30 N/mm² without sign. This makes their effect directly comparable to the effect of the bending of the crossbeam.

244

The results for the beam types with the standard span show for $w = 275$ a reduction of the stresses to 10.6% in comparison to the value for $w = 75$. The result for $H = 1400$ is approximately 44.4% of the value for $H = 600$. This means that larger cope holes have a more favorable effect than higher crossbeams.

With respect to the deeper beams the same procedure can be followed as for bending. The shear forces increase which reduces the effect of higher webs. Now the results for $H = 1400$ are approximately 80.3% of the results for $H = 600$, wheras the effect of the cut outs remains the same. It may be concluded that widening the cut outs gives the largest reduction of the stresses.

From the tables and figures the following conclusions can be drawn:
1. A wider cut out leads to lower stresses in the supports of the legs of the frame T_{lt} and T_{rt}.
2. Deeper crossbeams show lower stresses in the supports of the legs T_{lt} and T_{rt} though a full use of the beam adapted to the bending moment capacity reduces the favorable effect of enlarging the crossbeam depth.

If the leg length n in the frame schematization, see Fig. 19c, is increased the deflections will increase to a factor n as well, which means that the generated bending moment and normal force in location T_r for an imposed displacement will decrease accordingly.

7   Local in plane behaviour of crossbeam web

As shown in Chapter 5, the bending of the crossbeam generates both tension forces and secondary bending in the T-beam. The shear in the crossbeam generates bending and shear in the tooth and the T-beam. The vertically applied external loads on the deck cause normal forces with an eccentricity that generate stresses as well. Leendertz et al [4] showed the stress patterns in the full scale test specimen.
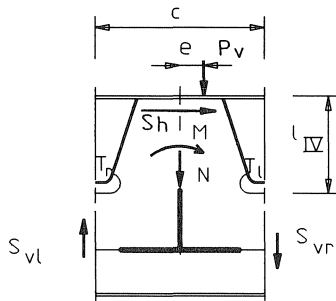

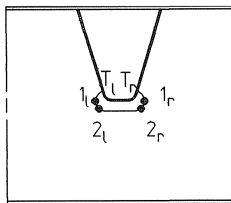*Fig. 30.   Schematization of forces is crossbeam web.*

Fig. 31.   Relevant stress locations crossbeam web.

Fig. 30 shows the section forces on this part of the crossbeam. Fig. 31 shows the locations of the web that are strongly affected by the secondary behaviour. Further studies are needed to find the influence of the frame structure which arises due to the fact that a simple antimetric system does not apply anymore as a schematization. The nominal stresses acting in location 1 (Fig. 31) due to the force P_v and the bending moment caused by P_v and S_h (Fig. 30) can be described as follows. Horizontal shear force S_h:

$$S_h = \frac{2 \cdot S_{vr} \cdot 0.5c + P_v \cdot 0.5}{a_1} \qquad (40)$$

Stresses in location 1:

$$\sigma_1 = \frac{S_h \cdot (l_{IV} - 0.5 \cdot d_c)}{W_{tooth}} + \frac{N}{A_{tooth}} \cdot e \qquad (41)$$

The eccentricity effect "e" needs further investigation as mentioned in Chapter 5. In location 1 the fatigue behaviour is governed by the stresses caused by bending of the tooth and, if present, the vertical external loads in the tooth. For every cut out in a crossbeam these effects interact with a

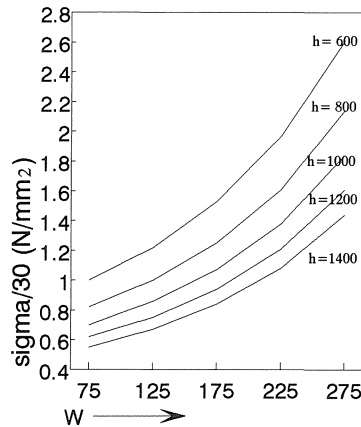| w	$H = 1400$	$H = 1200$	$H = 1000$	$H = 800$	$H = 600$
75	0.55	0.62	0.7	0.82	1
125	0.67	0.75	0.86	1	1.22
175	0.84	0.94	1.07	1.25	1.53
225	1.08	1.21	1.38	1.61	1.97
275	1.44	1.61	1.84	2.14	2.61

Fig. 32. Relative nominal stresses caused by bending due to S_h.

different magnitudes as they are caused by crossbeam bending and crossbeam shear, as described in Chapter 6.4. In the "Haibach" cut out this location governs the fatigue strength of the cut out. In the cut out with an oval shape generally location 2 is the most important one, due to the interaction of bending and shear of the tooth in combination with the crossbeam bending in the T-beam by the lever system and bending respectively shear caused by the Vierendeel actions in the T-beam.

Fig. 32 shows the relative nominal stresses in location 1 for bending due to S_h with the crossbeam with $H = 600$ and $w = 75$ as a reference. In this simpified approach widening the cope holes has a progressive unfavorable effect and enlarging the web height has a diminishing reduction effect on the stress levels in the narrowest section of the crossbeam tooth.

The stress concentration factor that shall be taken into account depends to a large extent on the corner radius of the cope hole. This means that the nominal stresses can not be the basis of specific conclusions on the (hot spot) stresses.

8   Out of plane behaviour

External loads applied on the deck between the crossbeams cause rotations and clamping moments in the supports of the stiffeners. These clamping moments act both in the web of the crossbeam and in the wall of the trough in case of a cut out with a cope hole. In the absence of a cope hole the bottom of the trough is connected to the web as well.
At this location bending moments will occur too. The level and the amount of load intervals caused by traffic, leads in some cases to cracks at these locations.

In this particular case it means that the web of the crossbeam is rotated by the stiffener. The reacting forces that occur depend on the geometry and the stiffness of the web as well as on the stiffness of the bottom flange.

It is not easy to find an adequate simplification for this bending problem as all elements involved consist of plates.
The chosen approach, which is shown in Figs. 33 and 34 is the following: The part of the web between the troughs is divided into an upper part which is supposed not to take part in the statical system and a lower part which is schematized into a horizontal beam (B1) between the two troughs. Further the web between the troughs and the web below the troughs is schematised as a vertical beam (B2), supported by the deckplate, a horizontal (B1) and the bottom flange of the crossbeam. In the analyses below the bottomflange is considered rigidly supported in the horizontal direction. Acting so a rotation of two adjacent troughs causes bending in the two beams. Special attention must be paid to the part below the troughs. In the case of a cope hole no immediate connection can be assumed between the bottom of the trough and the bottom flange. In the absence of cope holes however, a third beam (B3) connects the bottom of the trough to the bottom flange. Where no cope holes are present, the Beam1-Beam2 system is still assumed having the same effective widths and consequently the same structural properties. For Beam3 the width of the cut out with a cope hole is taken as the effective width for Beam3. The connection of Beam1 to the troughs can be considered as clamped due to the clamping influence of the bottom of the trough. Beam2 is considered to be supported by a hinge at the level of the deckplate, Beam1 and the bottom flange by are connected by

a hinge. Beam3, if present, is considered to be clamped to the bottom of the trough and hinge connected to the bottom flange.

It is possible to derive the spring stiffness for the structure formed by Beam1 and Beam2 at the connection of the bottom flange. Fig. 34 shows how the system B1B2 is linked to the system B3 by means of the crossbeam flange.
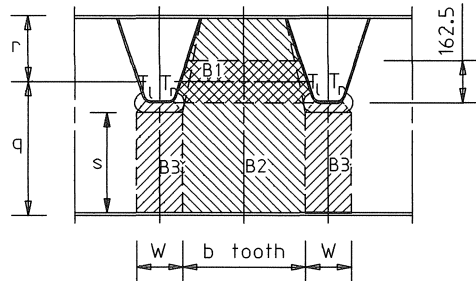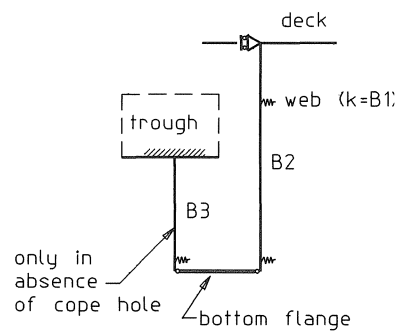

Fig. 33. Structural system out of plane behaviour.
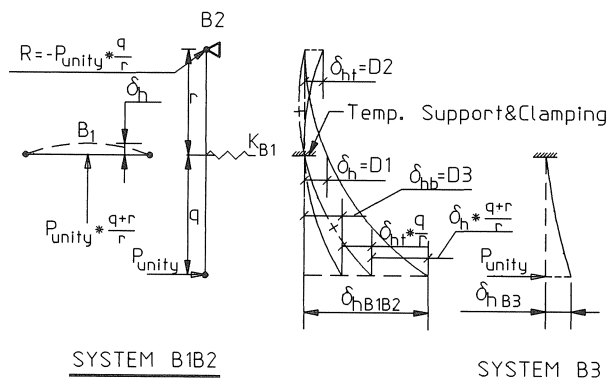

Fig. 34. System B1B2 and system B3.

Fig. 35. Deflections of elements in the systems B1B2 and B3.

248

Fig. 35 shows the deflections of the elements in the systems B1B2 and B3. The deflection of the center of B1, due to a unity P_{unity} on the lower end of B2 is:

The clamping moment M_{cw} in the web at T_{rw} and T_{lw} is:

$$M_{cw} = \frac{r+q}{q} \cdot \frac{P_{unity\,1} \cdot r}{8} \tag{42}$$

If for computation purposes B2 is temporarily clamped at the connection of Beam1, the free deflections of B2 at locations top and bottom can be computed:

The reaction force P_t at the top is:

$$P_t = P_{unity} \cdot \frac{q}{r} \tag{43}$$

$$\delta_h = \frac{r+q}{q} \cdot \frac{P_{unity\,1} \cdot p^3}{192 \cdot E \cdot I_{B1}} = D1 \tag{44}$$

The deflection $D2$ of the top is:

$$\delta_{ht} = \frac{P_{unity\,1} \cdot q \cdot r^2}{3 \cdot E \cdot I_{B2}} = D2 \tag{45}$$

The deflection $D3$ of the bottom can be determined as follows:

$$\delta_{hb} = \frac{P_{unity\,1} \cdot q^3}{3 \cdot E \cdot I_{B2}} = D3 \tag{46}$$

The total deflection of the bottom location of Beam2 follows from:

$$\delta_{hB1B2} = \frac{q+r}{r} \cdot D1 + \frac{q}{r} \cdot D2 + D3 \tag{47}$$

The spring constant K_{B1B2}, which substitutes the system B1B2 at the connection to the bottom flange is found by:

$$K_{B1B2} = \frac{P_{unity}}{\delta_{hB1B2}} \tag{48}$$

In the same way the spring constant K_{B3}, substituting the system B3 can be derived, under the assumption that the web is rigidly clamped in the trough:

The horizontal deflection D4 of the lower end of the cantilever loaded by a force P_{unity} will be:

$$\delta_{hB3} = \frac{P_{unity\,2} \cdot s^3}{3 \cdot E \cdot I_{B3}} = D4 \tag{49}$$

The clamping moment M_{cb} at the support of the trough bottom is:

$$M_{cb} = P_{unity\,2} \cdot s \tag{50}$$

The spring constant K_{B3} can be determined as follows:

$$K_{B3} = \frac{P_{unity}}{\delta_{hB4}} \tag{51}$$

In real structures often the bottom flange of the crossbeam will act as an elastic foundation. If the crossbeam is submitted to a symmetrical out of plane loading, a spring constant which substitutes the crossbeam flange support can easily be determined. However in may cases the real structure behaves more complex.

If the crossbeam flange is considered to be rigid, the highest clamping moments will be found. The following analyses are based on this assumption.

Based on a unit rotation ($\phi = 0.001$) of the troughs and taking $H = 600$ $w = 75$ as a reference the following relationship between the force transmitted by the system and generating clamping moments in the connection to the trough wall and the trough bottom can be found. Further these forces can be broken down into the contributions of the systems B1B2 and B3. In the case of cut outs B3 is not present.

For the analysed structures it is not easy to find the hot spot stresses at the locations T_{lw}, T_{rw} and T_{bw}, since stress concentration effects are involved, but based on some assumptions a computation of the nominal stresses can be carried out.

The following procedure has been followed:
1. Every B1-beam has an effective width of 162.5 mm
2. The effective width of the B3-beam for $w = 175$ at the connection is the width of the trough bottom which amounts 105 mm. With respect to the imaginairy troughs for the other cut outs the following factors apply to determine the resistance moment of the connection T_{bw}:

Table 3. Effective with factors for trough bottom to crossbeam web connection T_{bw}.

Width of cut out (cope holes included)	Factor of effective width of connection trough-web
$w = 75$	0.0095
$w = 125$	0.5144
$w = 225$	1.0000 (reference)
$w = 225$	1.4930
$w = 275$	1.9050

The results related to the unit forces P_{unity} can be transferred to forces related to a rotation of the troughs of 0.001 rad. Subsequently they can be processed in such a way that clamping moments are found in T_{lw}, T_{rw} and T_{bw}. When these clamping moments are divided by the appropriate resistance moment "W" the nominal bending stresses in the web of the crossbeam are found. These nominal stresses can only be used to investigate tendencies as they do not incorporate the full behaviour in detail with the appropriate concentration factors and are based on the assumption that the bottom flange of the crossbeam is rigidly supported with respect to out of plane movements.

Fig. 36 shows the relevant locations (T_{lw}, T_{rw} and T_{bw}) and Fig. 37 shows the value.

NOMINAL BENDING STRESSES IN THE CONNECTIONS TROUGH TO CROSSBEAM WEB (+/-)
(In case of cope holes the values in the B1B2 system are the only values that apply)

T_{rw}, T_{lw} Nominal bending stresses in crossbeam web due to forces transmitted by system B1B2
T_{bw} Nominal bending stresses in crossbeam web due to forces transmitted by system B3
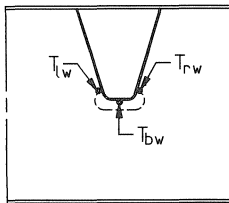   (all calculated stress results for T_{bw} have been divided by 1000)

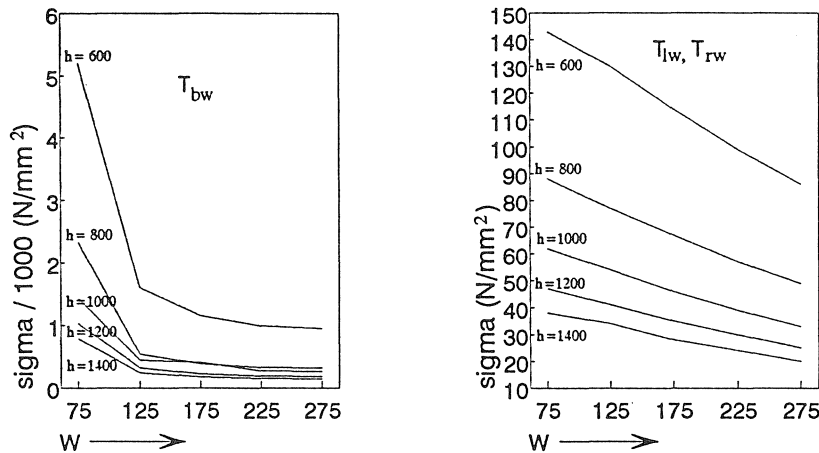Fig. 36. Locations T_{lw}, T_{rw} and T_{bw} of stresses due to out of plane rotations.

Fig. 37. Nominal stresses due to out of plane rotations ($\phi = 0.001$ RAD.) in T_{lw}, T_{rw} and T_{bw}.

251

The conclusions can be:

1. The stresses that occur in the connection of the trough bottom are 10 to 30 times higher than the stresses in the connection of trough wall. So, where large out of plane rotations are to be expected, a cope hole may be a more favorable solution.
2. The larger the web, the smaller the bending stresses in the connections.
3. The wider the cut out, the smaller the bending stresses in the connections.

The schematization as described above has been used in the analyses of the 4th Phase ECSC-research [4] test specimen and showed a in spite of a rough determination of the stress concentration factors, a good compliance with the results from FE-analyses and strain gauge measurements.

In the 3rd Phase ECSC fatigue tests, the out of plane bending was a substantial effect in the investigated connection between the trough and the crossbeam web. The numerical and analytical computations have been presented in [4]. The analyses as presented in this chapter show that the trough to crossbeam web connections (here comparable to beams with $w = 75$) with v-shaped stiffeners will have higher stresses than the trough to crossbeam connections with trapezoidal stiffeners, assumed that the structures and their boundary conditions are approximately identical. The connections with V-shaped stiffeners showed a much shorter fatigue life that the connections with trapezoidal stiffeners, which result is in line with the stress results as presented in Fig.36.

9 Overview of investigations and need for further work

9.1 Investigated locations

In many cases the results obtained in the previous chapters for the different mechanical phenomena coincide in the same locations. Taking an arbitrary trough to crossbeam connection at a distance "x" from midspan in a simply supported crossbeam an overview of the results for all locations will be presented. In addition will be indicated the need for further work. Fig. 38a and 38b show the relevant locations in side views of the crossbeam and the right side of the trough respectively, which have been subject of the analyses presented before. In addition the locations 1 and 2 have been modified in 1_l, 1_r, 2_l and 2_r.

Fig. 38c shows the stresses σ_{bh} at T_{lt} and T_{rt} caused by horizontal displacements due to crossbeam bending. Depending on the crossbeam bending moment, downward or upward, and the level of the neutral axis the stresses will be tension or compression. In the analyses described in Chapter 6.2 the stresses at the outer side are tension but for beam $H = 1400$.

Fig. 38d shows the stresses $\sigma_{b\phi}$ caused by section rotations at T_{lt} and T_{rt} due to crossbeam bending. depending on the crossbeam bending moment, upward or downward they wil be tension of compression. In all beams analysed in Chapter 6.2 the stresses at the outer side are tension.

Fig. 38e shows the stresses σ_s caused by vertical diplacements at T_{lt} and T_{rt} due to crossbeam shear. The analyses as described in Chapter 6.3 with the load arrangement as in Fig. 38a lead to compressive stresses in T_{lt} and tensile stresses in T_{rt}, in both locations of equal magnitude.

Fig. 38f shows the stresses σ_{pn} due to contraction of the trough by bending moments in the trough as described in "Secondary Stresses in Closed Orthotropic Deck Ribs at Floor Beams" [ref. 2]. As the analyses presented here were limited to the crossbeam behaviour. In real structures these stresses will show fluctuations and change of sign depending on the rigidity of the trough stiffeners and the crossbeams.

Fig. 38. Overview of investigated locations and relation to mechanical models.

In addition to all locations mentioned before, locations T_{lwf}, T_{lwr} (not shown), T_{rwf} and T_{rwr} are introduced. In these locations The carry-over effect from trough to crossbeam web of local restraining forces and bending moments due to Crossbeam in plane behaviour and contraction of the trough are induced. Further the locations T_{ltf}, T_{ltr} (not shown), T_{rtf} and T_{rtr} are introduced. In these locations the carry-over effect from the crossbeam out of plane behaviour causes out of plane bending in the trough web.

9.2   Combination of stresses in trough web

In the case of a simple span, loaded by an equally distributed load, the bending diagram will be a parabola with the maximum value at midspan and the shear force diagram will be linear with maximum values at the supports and "0" at midspan, as shown in Fig. 39.

In the previous chapters the stresses at T_{lt} and T_{rt} have been computed for the crossbeam bending effect and the crossbeam shear effect.
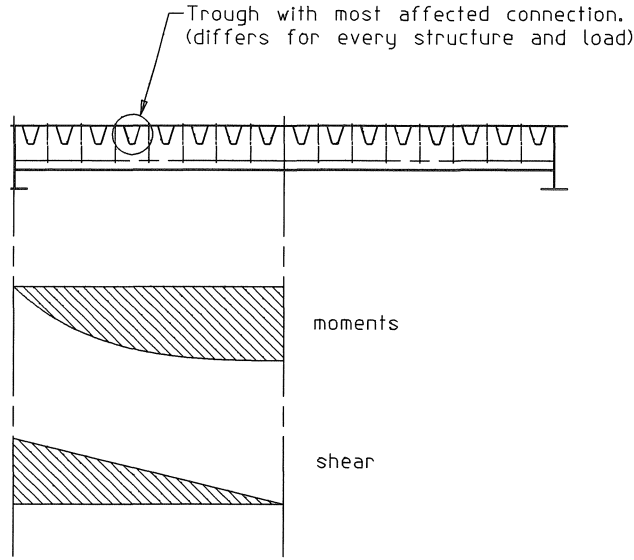
Fig. 39. Combination of stresses in trough web.

At a distance "x" from midspan the crossbeam bending effect (stresses in T_{lt} and T_{rt}) will be reduced by a factor r_b:

$$r_b = \left(1 - \frac{4}{l^2} \cdot x^2 \right) \tag{52}$$

At a distance "x" from midspan the crossbeam shear effect (stresses in T_{lt} and T_{rt}) will be increased by a factor r_s:

$$r_s = \frac{2}{l} \cdot x \tag{53}$$

If the stresses at T_{lt} and T_{rt} due to crossbeam bending are called σ_{bh}, $\sigma_{b\phi}$, due to crossbeam shear are called σ_s, and the stresses due to contraction are σ_{pn} and the combination of the stresses is called σ_c, the stresses in a trough at a distance "x" from midspan due to bending and a positive shear force become at T_{lt}:

$$\sigma_c = (\sigma_{bh} + \sigma_{b\phi}) \cdot \left(1 - \frac{4}{l^2} \cdot x^2 \right) - \sigma_s \cdot \frac{2}{l} \cdot x \cdot \sigma_{pn} \tag{54}$$

The combined stresses at location T_{rt} become::

$$\sigma_c = (\sigma_{bh} + \sigma_{b\phi}) \cdot \left(1 - \frac{4}{l^2} \cdot x^2 \right) + \sigma_s \cdot \frac{2}{l} \cdot x \cdot \sigma_{pn} \tag{55}$$

254

The troughs which are most critically affected by the bending and shear behaviour can be found, where σ_c has a maximum value.

This procedure is not carried out here, as these results have no practical value. All results are only comparative and do not include the effects of locally introduced loads as described before in Chapter 5.

9.3 *Need for further work*

The influence of external applied loads will have to be studied more extensively to develope simple analytical models which describe their influence in the relevant stress locations.

All stresses computed above are nominal stresses. In order to enable the determination of hot spot stresses, for all locations appropriate stress concentration factors will have to be determined.

10 Conclusions and remarks

– The analyses of the in plane bending behaviour of the crossbeam show that the bending is not much affected by the cut outs and cope holes. With respect to deflections the effect of the cut outs can be transferred into an equivalent bending stiffness ratio c_b.

– The analyses of the in plane shear behaviour of the crossbeam show a large influence from the cut outs and cope holes. With respect to the deflections can be transferred into an equivalent shear stiffness ratio c_s.

– The schematizations used to determine the equivalent bending and shear stiffnes ratios show the transfer of bending and shear in the structure and can be used to determine with a simple method the relative displacements and rotations of the lower ends of the connection between trough and crossbeam web T_l and T_r.

– The relative displacements and rotations represent the imposed deformations on the trough. Their effects, being section forces and section moments, in the trough can be computed by simple frame schematizations. Accordingly nominal stresses can be computed.

– The schematization for crossbeam shear can be used to analyse the crossbeam web between the cope holes. However eccentric loadings could not yet been schematized in a simple model.

– The out of plane bending of the crossbeam, generated by induced rotations of the trough stiffeners about the longitudinal axis of the crossbeam, can be schematized in a simple model, which gives a clear insight in the transfer of loads. In comparison with an FE-model it showed to be a fairly reliable description of the structural behaviour. The results explained differences in fatigue test results of various details.

– The results show, that due to different level of the contribution of each phenomenon investigated above, no standard cut out with cope hole exists which deals in an optimal way with all effects.

11   Definitions and abbreviations

11.1   Definitions

Deck	–	Steel plating which carries the surfacing and traffic loads.
Stiffeners	–	Longitudinal Elements which act together with the deck plate as longitudinal beams.
Crossbeam	–	Structural beam element which transfers dead loads and traffic loads from a deck structure to the maingirders.
Cut Out	–	Parts of the crossbeam where material has been removed to enable continuous stiffeners passing through the crossbeam.
Cope Hole	–	Extension of the cut out to facilitate easy fitting of the stiffeners.
T-beam	–	Remaining part of the crossbeam below a stiffener - crossbeam connection with a cope hole.

11.2   Abbreviations

A	Area of section
A_{tooth}	Cross section area of tooth
a_l	Lever arm betweem deck and T-beam
$B''NR''$	Beam Type in beam schematization out of plane bending
b	Width of section, length of horizontal leg in half frame schematization of trough bottom
c	Centre to centre distance of trough stiffeners
c_b	Equivalent bending stiffness ratio of crossbeam
c_s	Equivalent shear stiffness ratio of crossbeam
$D1$	Influence horizontal deflection of Beam1 (B1) by a unit force (P_{unity}) at the lower end of Beam 2 (B2).
$D2$	Hor. deflection as cantilever at top of Beam2 by equilibrium force of P_{unity1}
$D3$	Hor. deflection as cantilever at bottom of Beam2 by P_{unity}
$D4$	Hor. deflection of Beam3 By P_{unity}
d_c	Diameter of cope hole in crossbeam Web
δ_h	Horizontal displacement
δ_{hB1}	$D1$
δ_{hB1B2}	Horizontal displacement of system B1B2 due to a unit force
δ_{hB3}	$D4$
δ_v	Vertical displacement
δ_{vP}	Vertical displacement due to external vertical load P
$\delta_{v\text{-}add}$	Additional vertical displacement caused by horizontal deflections of tooth
$\delta_{v\text{-}full}$	Vertical displacement of crossbeam with full web due to shear force
E	Modulus of elasticity
e	Eccentricity
F_{hA}	Horizontal normal force in bottom flange left side
F_{hB}	Horizontal normal force in bottom flange right side
f	Horizontal projection of leg in trapezoidal frame schematization of trough
ϕ	Rotation

ϕ_1	Rotation in Part I
ϕ_2	Rotation in Part II
ϕ_A	Rotation in Section A
ϕ_B	Rotation in Section B (location T_r) by crossbeam bending
$\phi_{A\text{-}cutout}$	Rotation in Section A in crossbeam with cut outs
$\phi_{A\text{-}full}$	Rotation in Section A in crossbeam without cut outs
g	Vertical projection of leg in trapezoidal frame schematization of trough
I_{full}	Moment of inertia of crossbeam without cut outs
I_{frame}	Moment of inertia of frame elements in trough shematization
$I_{T\text{-}beam}$	Moment of inertia of T-beam
K	Spring constant (P/δ)
K_{B1B2}	Spring constant, substituting behaviour of Beam1 and Beam2
K_{B3}	Spring constant, substituting behaviour of Beam3
l	Span length
M	Moment
M_{cb}	Clamping moment in trough bottom due to out of plane behaviour
M_{cw}	Clamping moment in trough wall due to out of plane behaviour
M_{lever}	Part of the crossbeam section bending moment distributed to the lever system
M_{unity}	Unity bending moment
$M_{T\text{-}beam}$	Part of the crossbeam section bending moment distributed to the T-beam
N	Normal force in section
n	Leg of trapezoidal frame schematization of trough
P	Force
P_h	Horizontal force
P_v	Vertical force
P_{unity}	Unit force on system B1B2
P_{unity}	Unit force on system B3
p	Distance B1 to deck
q	Distance B1 to bottom flange
R_l	Lever system ratio
R_T	Lever system ratio
r	Distance trough bottom to bottom flange
S	Shear force
S_h	Horizontal shear force
S_v	Vertical shear force
S_{vl}	Vertical shear force left side
S_{vr}	Vertical shear force right side
σ	Normal stress
σ_b	Stress in trough wall due to crossbeam bending
σ_{bh}	Stress in trough wall due to horizntal translations caused by crossbeam bending
$\sigma_{b\phi}$	Stress in trough wall due to section rotations caused by crossbeam bending
σ_s	Stress in trough wall due to crossbeam shear
σ_{pn}	Stress in trough wall due to contraction of trough stiffener by trough bending

T_b	Connection of trough bottom to crossbeam Web
T_{bw}	Connection of trough bottom to crossbeam web location in crossbeam web
T_l	Lower end of connection trough to crossbeam web
T_{lt}	Lower end of connection trough to crossbeam web, location in trough left side
T_{ltf}	Lower end of connection trough to crossbeam web, location in trough left side front
T_{ltr}	Lower end of connection trough to crossbeam web, location in trough left side rear
T_{lw}	Lower end of connection trough to crossbeam web, location in crossbeam web
T_{lwf}	Lower end of connection trough to crossbeam web, location in crossbeam web front
T_{lwr}	Lower end of connection trough to crossbeam web, location in crossbeam web rear
T_r	Lower end of connection trough to crossbeam web
T_{rt}	Lower end of connection trough to crossbeam web, location in trough right side
T_{rtf}	Lower end of connection trough to crossbeam web, location in trough right side front
T_{rtr}	Lower end of connection trough to crossbeam web, location in trough right side rear
T_{rw}	Lower end of connection trough to crossbeam web, location in crossbeam web
T_{rwf}	Lower end of connection trough to crossbeam web, location in crossbeam web front
T_{rwr}	Lower end of connection trough to crossbeam web, location in crossbeam web rear
w	Length of cut out including cope hole
W	Resistance moment
W_1	Resistance moment beam type 1 H=600 w=75
W_n	Resistance moment beam type n
W_{tooth}	Resistance moment of tooth
1_l	Location 1 in crossbeam web left side
1_r	Location 1 in crossbeam web right side
2_l	Location 2 in crossbeam web left side
2_r	Location 2 in crossbeam web right side

12   References

1. FALKE J., Zum Tragverhalten und zur Berechnung von Querträgern orthotroper Platten. Thesis TU-Braunschweig 1983.

2. WOLCHUK R. and OSTAPENKO A., Secondary Stresses in Closed Orthotropic Deck Ribs at Floor Beams. ASCE Journal of Structural Engineering, Vol. 118, No.2, February 1992.

.3 KOLSTEIN M.H., WARDENIER J. and LEENDERTZ J.S., Fatigue Performance of the Trough to Crossbeam Connection in Orthotropic Steel Bridge Decks. Nordic Steel Conference Malmö 1995.

4. LEENDERTZ J.S., WARDENIER J. and KOLSTEIN M.H., Numerical Analyses of the Trough to Crossbeam Connections in Orthotropic Steel Decks. Nordic Steel Conference Malmö 1995.

5. KOLSTEIN M.H., LEENDERTZ J.S. and WARDENIER J., Fatigue Design Aspects of Orthotropic Steel Bridges. First European Conference on Steel Structures "Eurosteel '95", Athens 1995.

6. PELIKAN W. and ESSLINGER M., Die Stahlfahrbahn – Berechnung und Konstruktion. M.A.N.-Forschungsheft Nr. 7/1957.

7. HAIBACH E. and PLASIL I., Untersuchungen zur Betriebsfestigkeit von Stahlleichtfahrbahnen mit Trapezhohlsteifen im Eisenbahnbrückenbau. Der Stahlbau 9/1983

8. MANG F., BUCAK Ö. and KARCHER D., Fatigue of Orthotropic Steel Bridge Decks. Proceedings of the 3rd International Conference on Steel and Aluminium Structures, MAS Printing Co. Istanbul 1995.

9. Design Manual for Orthotropic Steel Plate Deck Bridges.
   American Institute of Steel Construction, New York 1962.

10. LEHRKE, H.P., Fatigue Tests on Large Size Specimens of Stiffener to Crossbeam Connection. Proceedings IABSE Workshop Remaining Fatigue Life of Steel Structures, Lausanne 1990.

11. LEENDERTZ J.S., KOLSTEIN, M.H., The Behaviour of Trough Stiffener to Crossbeam Connections in Orthotropic Steel Bridge Decks, Delft University of Technology, Stevin Report 6-95-16, Delft 1995.